Hybrid Strategy to Achieve 3D Base Isolation of Structures

(Article begins on next page)

01 September 2025

HYBRID STRATEGY TO ACHIEVE 3D BASE ISOLATION OF STRUCTURES

M. Domaneschi [1], L. Martinelli [2], G.P. Cimellaro [3]

[1] *Assistant Professor, Politecnico di Torino DISEG, marco.domaneschi@polito.it*
[2] *Associate Professor, Politecnico di Milano DICA, luca.matinelli@polimi.it*
[3] *Associate Professor, Politecnico di Torino DISEG, gianpaolo.cimellaro@polito.it*

Abstract

Some aspects, related to the 3D base isolation of structures to control the effects of both the horizontal and vertical components of ground motion, are presented in this paper. A massive structure (a Nuclear Power Plant building) equipped with a traditional horizontal base isolation system is numerically studied. The base isolation system uses rubber bearings (low and high damping) coupled with a tuned mass damper (TMD) in the vertical direction. Possible positive and negative aspects from the implementation of the proposed hybrid strategy are investigated.

Numerical analyses show that the presence of the TMD mitigate the vertical effects of the three-dimensional ground motion coupled with the elastomeric bearings, reducing both the vertical and the horizontal absolute acceleration in the superstructure under certain conditions. Vertical acceleration in the superstructure appears related to the horizontal motion, due to the building's centroid position that induces rocking.

Keywords: Hybrid, TMD, rubber bearings, damping

1. Introduction

Seismic base isolation to mitigate the horizontal seismic response of a structure has by now become a mature and well established strategy [1-3]. It consists in the insertion of specifically designed deformable devices (isolation bearings) within an interface between the structure to be controlled (the superstructure) and the foundation slab to shift the fundamental period of the superstructure above the predominant period of the ground motion.

The standard implementation of base isolation is focused on the lateral movement mitigation of the superstructure, and, therefore, employs laterally flexible isolators to shift the superstructure fundamental period typically in the range from 2 to 4 seconds. Besides, since the isolation effect is performed at the costs of large horizontal relative displacements between the foundation and the superstructure, a form of energy hysteretic damping (energy dissipation) is usually implemented to control such effects. Base Isolation with respect to the lateral motion has been the subject of a vast amount of published research and has become an accepted and standardized approach in several seismic design codes (e.g. [4]).

The concept of controlling the vertical motion in seismic isolated systems has, instead, received much less attention. The first proposals were mainly based on mechanical devices. Full-scale tests on shaking tables pointed out a less satisfactory performance than that associated, at the time, to horizontal isolation.

More recently, the idea of controlling the vertical motion of a building has surfaced again in relation to the protection of Nuclear Power Plants (NPPs). Isolation in vertical direction, coupled to horizontal base isolation, is known in the nuclear community also as "3D isolation". Control of the vertical motion can be implemented either by using integrated isolation solutions, in which a single device provides isolation with respect to all three ground motion components, or by adding a localized vertical isolation component, or damping, in series to a device that provides isolation with respect to the horizontal motion components [5,6]. In this work, the vertical motion is controlled by selectively tune TMDs active in vertical direction, which are also beneficial in reducing the rocking motion.

2. Methodology

An integrated isolation solution for a NPP is herein dealt with and consists in elastomeric bearings. Such rubber isolators can be classified as Low Damping Rubber Bearings ((LDRBs) or High Damping Rubber Bearings (HDRB), depending on the damping capabilities of the rubber they are made of. The stiffness and energy dissipation of high damping bearings is highly nonlinear and depends on the level of shear strain. The effective damping of these devices can reach 10 to 15 % of the critical. The low damping bearings exhibit an almost linear characteristic with damping values in the range of 2 to 5 % of critical in the lateral direction. These values decrease if the vertical direction is analyzed. These typologies are both considered in this preliminary study.

This work focuses first on the vertical motion of the superstructure and on providing the required amount of damping in the vertical direction by means of a properly tuned Tuned Mass Damper (TMD). Then we focus on a complete 3D representation of the NPP building and base isolation system (Figure 1) to analyze the way to mitigate the rocking motion and the vertical seismic response.
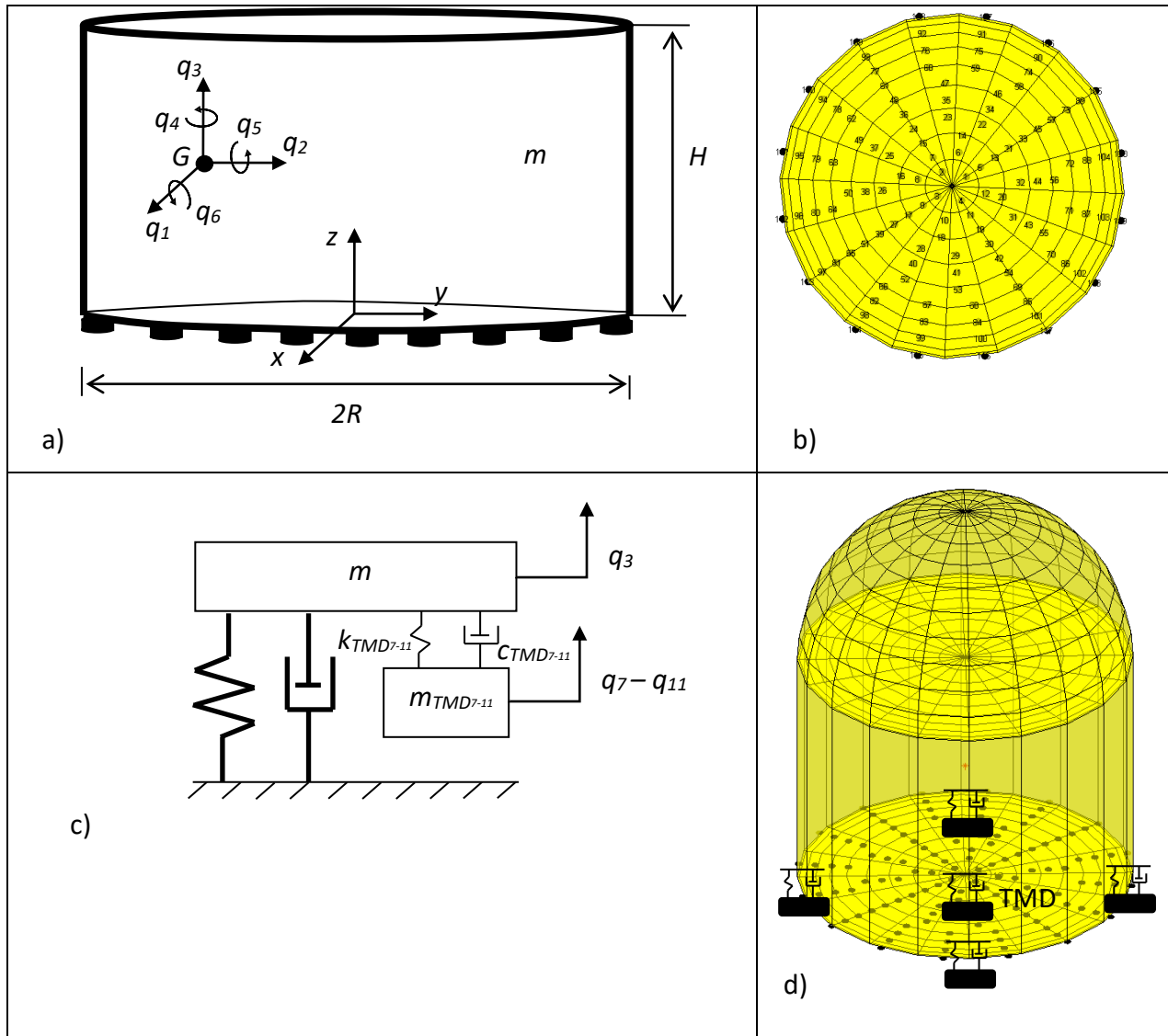
2

Figure 1: a)-d) Simplified model of the NPP building and location of the TMDs. c) Linear dynamic model for the vertical motion of the superstructure with mass *m* and the TMD.

The Tuned Mass Dampers used to passively control the superstructure consist in a mass attached to the superstructure with a spring and a damper (Figure 1c). The control exerted by the TMDs can be classified as passive, since the TMDs work as passive energy dissipation devices, providing the damping required to control the vertical motion. The damper in the TMD dissipates energy whenever the mass of the TMD oscillates relatively to the superstructure. In order to ensure this motion, the TMD is carefully tuned so that its natural frequency is close to one relevant frequency of the base isolated system. The energy transferred from the superstructure to the TMD generates large oscillations of the mass of the TMD, to the point that this aspect can become a limiting one in the design of the TMD.

Due to the quasi-resonance required between the controlled mode of the base isolated system and the TMDs, required for having an effective control, the TMDs operates efficiently only in a narrow frequency band. That is the frequency of the harmonic input or, in case of wide frequency input, the main natural frequency of the structure. Therefore, the TMDs mitigates only the vibration mode it are tuned to [7].

3

One of the earliest theory for the design of TMD was presented by Den Hartog in his well-known book [8], where the optimal parameters (natural frequency and damping ratio) of a TMD that minimizes the displacement of the primary structure (here the superstructure) where obtained by means of the so called fixed-points method. The primary structure is supposed to have vanishing structural damping. Optimal parameters for a wider list of minimization objectives, also obtained by the fixed-points method, were later reported in [9], also for vanishing damping of the primary structure. Empirical formulas for several minimization objectives were given by Ioi and Ikeda [10] while approximate, analytical closed-form, and series solution for the case of non-vanishing damping of the primary structure can be found in [11] for mono-frequency and white noise input.

Optimization of the TMDs parameters in the case of earthquake type excitation was presented in [12] for an earthquake excitation modelled by a stationary stochastic process with a power spectral density of the Kanai-Tajimi type [13, 14]. By properly selecting the frequency ω_g and damping ζ_g of the Kanai-Tajimi filter, different spectral density shapes can be represented. For fitting of real earthquake accelerations it has been found that the frequency ω_g has to be in the range 3-12 Rad/s. The value of the frequency ω_g and the damping ζ_g associated to the EC8 [4] elastic response spectra can be found in [15, 16], along with a closed form expression for the elastic response spectra derived from this PSD.

3. Dynamic Equations of the base isolated IRIS-NPP equipped with five TMDs

The considered NPP building is the IRIS medium power (335 MWe) pressurized light water reactor whose preliminary design has been developed by an international consortium which includes more than 20 partners from 10 countries. In a tentative design, the introduction of an isolation system was considered; the system is made by 120 HDRB (High Damping Rubber Bearings) devices installed between the foundation slab and the base [2]. The isolators are made of alternated rubber layers and steel plates, bonded through vulcanization. Damping factors intrinsic to this technology ranges generally from 10% to 20%, while shear modulus lies in the 0.8–1.4 MPa range.

With reference to Figure 1a, the equations of motion of the 3D IRIS base isolated NPP model with 6 degrees of freedom are presented in the following (Equations 1-11) within a Lagrangian approach. The TMDs are active in the vertical direction and are applied one at the geometric center of the isolation plane and four at the extremities of the x and y axis of the same, in a cross-shape configuration.

Coordinates q_1, q_2, q_3 (parallel to the global reference system x, y, z) represent displacement components of the centroid of the main structure, while coordinates q_4, q_5, q_6 are rotations around respectively the q_3, q_2, q_1 directions. Coordinates $q_7 - q_{11}$ are the vertical displacement component of the TMD masses (Figure 1c).

The following equations of motion arise:

$$(m + \sum_i m_{TMDi})\ddot{q}_1 + \sum_{i=1}^{n} F_{f1i} = (m + \sum_i m_{TMDi})a_{h1} \tag{1}$$

$$(m + \sum_i m_{TMDi})\ddot{q}_2 + \sum_{i=1}^{n} F_{f2i} = (m + \sum_i m_{TMDi})a_{h2} \tag{2}$$

4

$$(m + \sum_i m_{TMDi})\ddot{q}_3 + k_v n q_3 - k_v \sum_{i=1}^n (x_i - x_G) q_5 + k_v \sum_{i=1}^n (y_i - y_G) q_6 +$$

$$+ c_v n \dot{q}_3 - c_v \sum_{i=1}^n (x_i - x_G) \dot{q}_5 + c_v \sum_{i=1}^n (y_i - y_G) \dot{q}_6 -$$

$$- k_{TMD1}(q_7 - q_3 + (x_{TMD1} - x_G) q_5 - (y_{TMD1} - y_G) q_6) -$$

$$- k_{TMD2}(q_8 - q_3 + (x_{TMD2} - x_G) q_5 - (y_{TMD2} - y_G) q_6) -$$

$$- k_{TMD3}(q_9 - q_3 + (x_{TMD3} - x_G) q_5 - (y_{TMD3} - y_G) q_6) -$$

$$- k_{TMD4}(q_{10} - q_3 + (x_{TMD4} - x_G) q_5 - (y_{TMD4} - y_G) q_6) -$$

$$- k_{TMD5}(q_{11} - q_3 + (x_{TMD5} - x_G) q_5 - (y_{TMD5} - y_G) q_6) -$$

$$- c_{TMD1}(\dot{q}_7 - \dot{q}_3 + (x_{TMD1} - x_G) \dot{q}_5 - (y_{TMD1} - y_G) \dot{q}_6) -$$

$$- c_{TMD2}(\dot{q}_8 - \dot{q}_3 + (x_{TMD2} - x_G) \dot{q}_5 - (y_{TMD2} - y_G) \dot{q}_6) -$$

$$- c_{TMD3}(\dot{q}_9 - \dot{q}_3 + (x_{TMD3} - x_G) \dot{q}_5 - (y_{TMD3} - y_G) \dot{q}_6) -$$

$$- c_{TMD4}(\dot{q}_{10} - \dot{q}_3 + (x_{TMD4} - x_G) \dot{q}_5 - (y_{TMD4} - y_G) \dot{q}_6) -$$

$$- c_{TMD5}(\dot{q}_{11} - \dot{q}_3 + (x_{TMD5} - x_G) \dot{q}_5 - (y_{TMD5} - y_G) \dot{q}_6) = m a_v$$

(3)

$$(I_{G1} + \sum_i m_{TMDi}(x_{TMDi} - x_G)^2 + \sum_i m_{TMDi}(y_{TMDi} - y_G)^2)\ddot{q}_4 -$$

$$- \sum_{i=1}^n F_{f1i}(y_i - y_G) + \sum_{i=1}^n F_{f2i}(x_i - x_G) = 0$$

(4)

$$I_{G2}\ddot{q}_5 + z_G \left(\sum_{i=1}^n F_{f1i} \right) - k_v \sum_{i=1}^n (x_i - x_G) q_3 + k_v \sum_{i=1}^n (x_i - x_G)^2 q_5 - \left(k_v \sum_{i=1}^n (x_i - x_G)(y_i - y_G) \right) q_6 -$$

$$- c_v \sum_{i=1}^n (x_i - x_G) \dot{q}_3 + c_v \sum_{i=1}^n (x_i - x_G)^2 \dot{q}_5 - \left(c_v \sum_{i=1}^n (x_i - x_G)(y_i - y_G) \right) \dot{q}_6 +$$

$$+ k_{TMD1}(q_7 - q_3 + (x_{TMD1} - x_G) q_5 - (y_{TMD1} - y_G) q_6)(x_{TMD1} - x_G) +$$

$$+ k_{TMD2}(q_8 - q_3 + (x_{TMD2} - x_G) q_5 - (y_{TMD2} - y_G) q_6)(x_{TMD2} - x_G) +$$

$$+ k_{TMD3}(q_9 - q_3 + (x_{TMD3} - x_G) q_5 - (y_{TMD3} - y_G) q_6)(x_{TMD3} - x_G) +$$

$$+ k_{TMD4}(q_{10} - q_3 + (x_{TMD4} - x_G) q_5 - (y_{TMD4} - y_G) q_6)(x_{TMD4} - x_G) +$$

$$+ k_{TMD5}(q_{11} - q_3 + (x_{TMD5} - x_G) q_5 - (y_{TMD5} - y_G) q_6)(x_{TMD5} - x_G) +$$

$$+ c_{TMD1}(\dot{q}_7 - \dot{q}_3 + (x_{TMD1} - x_G) \dot{q}_5 - (y_{TMD1} - y_G) \dot{q}_6)(x_{TMD1} - x_G) +$$

$$+ c_{TMD2}(\dot{q}_8 - \dot{q}_3 + (x_{TMD2} - x_G) \dot{q}_5 - (y_{TMD2} - y_G) \dot{q}_6)(x_{TMD2} - x_G) +$$

$$+ c_{TMD3}(\dot{q}_9 - \dot{q}_3 + (x_{TMD3} - x_G) \dot{q}_5 - (y_{TMD3} - y_G) \dot{q}_6)(x_{TMD3} - x_G) +$$

$$+ c_{TMD4}(\dot{q}_{10} - \dot{q}_3 + (x_{TMD4} - x_G) \dot{q}_5 - (y_{TMD4} - y_G) \dot{q}_6)(x_{TMD4} - x_G) +$$

$$+ c_{TMD5}(\dot{q}_{11} - \dot{q}_3 + (x_{TMD5} - x_G) \dot{q}_5 - (y_{TMD5} - y_G) \dot{q}_6)(x_{TMD5} - x_G) = 0$$

(5)

5

$$I_{G3}\ddot{q}_6 + z_G\left(\sum_{i=1}^{n}F_{f2i}\right) + k_v\sum_{i=1}^{n}(y_i - y_G)q_3 - \left(k_v\sum_{i=1}^{n}(x_i - x_G)(y_i - y_G)\right)q_5 + k_v\sum_{i=1}^{n}(y_i - y_G)^2 q_6 +$$

$$+c_v\sum_{i=1}^{n}(y_i - y_G)\dot{q}_3 - \left(c_v\sum_{i=1}^{n}(x_i - x_G)(y_i - y_G)\right)\dot{q}_5 + c_v\sum_{i=1}^{n}(y_i - y_G)^2\dot{q}_6 -$$

$$-k_{TMD1}(q_7 - q_3 + (x_{TMD1} - x_G)q_5 - (y_{TMD1} - y_G)q_6)(y_{TMD1} - y_G) -$$

$$-k_{TMD2}(q_8 - q_3 + (x_{TMD2} - x_G)q_5 - (y_{TMD2} - y_G)q_6)(y_{TMD2} - y_G) -$$

$$-k_{TMD3}(q_9 - q_3 + (x_{TMD3} - x_G)q_5 - (y_{TMD3} - y_G)q_6)(y_{TMD3} - y_G) -$$

$$-k_{TMD4}(q_{10} - q_3 + (x_{TMD4} - x_G)q_5 - (y_{TMD4} - y_G)q_6)(y_{TMD4} - y_G) -$$

$$-k_{TMD5}(q_{11} - q_3 + (x_{TMD5} - x_G)q_5 - (y_{TMD5} - y_G)q_6)(y_{TMD5} - y_G) -$$

$$-c_{TMD1}(\dot{q}_7 - \dot{q}_3 + (x_{TMD1} - x_G)\dot{q}_5 - (y_{TMD1} - y_G)\dot{q}_6)(y_{TMD1} - y_G) -$$

$$-c_{TMD2}(\dot{q}_8 - \dot{q}_3 + (x_{TMD2} - x_G)\dot{q}_5 - (y_{TMD2} - y_G)\dot{q}_6)(y_{TMD2} - y_G) -$$

$$-c_{TMD3}(\dot{q}_9 - \dot{q}_3 + (x_{TMD3} - x_G)\dot{q}_5 - (y_{TMD3} - y_G)\dot{q}_6)(y_{TMD3} - y_G) -$$

$$-c_{TMD4}(\dot{q}_{10} - \dot{q}_3 + (x_{TMD4} - x_G)\dot{q}_5 - (y_{TMD4} - y_G)\dot{q}_6)(y_{TMD4} - y_G) -$$

$$-c_{TMD1}(\dot{q}_{11} - \dot{q}_3 + (x_{TMD5} - x_G)\dot{q}_5 - (y_{TMD5} - y_G)\dot{q}_6)(y_{TMD5} - y_G) = 0$$

(6)

$$m_{TMD1}\ddot{q}_7 + k_{TMD1}(q_7 - q_3 + (x_{TMD1} - x_G)q_5 - (y_{TMD1} - y_G)q_6) +$$
$$+c_{TMD1}(\dot{q}_7 - \dot{q}_3 + (x_{TMD1} - x_G)\dot{q}_5 - (y_{TMD1} - y_G)\dot{q}_6) = -m_{TMD1}a_v$$

(7)

$$m_{TMD2}\ddot{q}_8 + k_{TMD2}(q_8 - q_3 + (x_{TMD2} - x_G)q_5 - (y_{TMD2} - y_G)q_6) +$$
$$+c_{TMD2}(\dot{q}_8 - \dot{q}_3 + (x_{TMD2} - x_G)\dot{q}_5 - (y_{TMD2} - y_G)\dot{q}_6) = -m_{TMD2}a_v$$

(8)

$$m_{TMD3}\ddot{q}_9 + k_{TMD3}(q_9 - q_3 + (x_{TMD3} - x_G)q_5 - (y_{TMD3} - y_G)q_6) +$$
$$+c_{TMD3}(\dot{q}_9 - \dot{q}_3 + (x_{TMD3} - x_G)\dot{q}_5 - (y_{TMD3} - y_G)\dot{q}_6) = -m_{TMD3}a_v$$

(9)

$$m_{TMD4}\ddot{q}_{10} + k_{TMD4}(q_{10} - q_3 + (x_{TMD4} - x_G)q_5 - (y_{TMD4} - y_G)q_6) +$$
$$+c_{TMD4}(\dot{q}_{10} - \dot{q}_3 - (x_{TMD4} - x_G)\dot{q}_5 - (y_{TMD4} - y_G)\dot{q}_6) = -m_{TMD4}a_v$$

(10)

$$m_{TMD5}\ddot{q}_{11} + k_{TMD5}(q_{11} - q_3 + (x_{TMD5} - x_G)q_5 - (y_{TMD5} - y_G)q_6) +$$
$$+c_{TMD5}(\dot{q}_{11} - \dot{q}_3 + (x_{TMD5} - x_G)\dot{q}_5 - (y_{TMD5} - y_G)\dot{q}_6) = -m_{TMD5}a_v$$

(11)

where a "G" subscript denotes quatities relative to the centroid of the NPP building, while the following symbols apply: F_{f1_i} and F_{f2_i} are the horizontal restoring forces exerted by the *i-th* isolator; k_v, c_v are the isolator vertical stiffness and damping coefficients; $m, I_{G_1}, I_{G_2}, I_{G_3}$ are the mass and moments of inertia of the isolated portion of the building; $m_{TMDi}, k_{TMDi}, c_{TMDi}$ are the TMD mass, stiffness and damping coefficients of the *i*-TMD; a_{h1}, a_{h2}, a_v are the components of ground acceleration; x_{TMDi}, y_{TMDi} coordinated of the *i*-TMD; x_G, y_G are the coordinates of the centroid.

4. Preliminary unidirectional analysis on the base isolated IRIS-NPP with TMDs

The preliminary analysis of the NPP building has been performed focusing on the response in the vertical direction by the direct integration of the equation of motion of a simplified model of the NPP. The 2DOFS model in Figure 1c has been adopted to this end with the relevant parameters for the direction of motion in question as reported in [2]. The seismic input in the vertical direction has been fixed to 1g Peak Ground Acceleration (PGA) with the aim of possible generalizations due to the intrinsic linearity of the numerical model. The ground motion has been selected so that it is compatible to the USNRC 1.60 response spectra, as in [2].
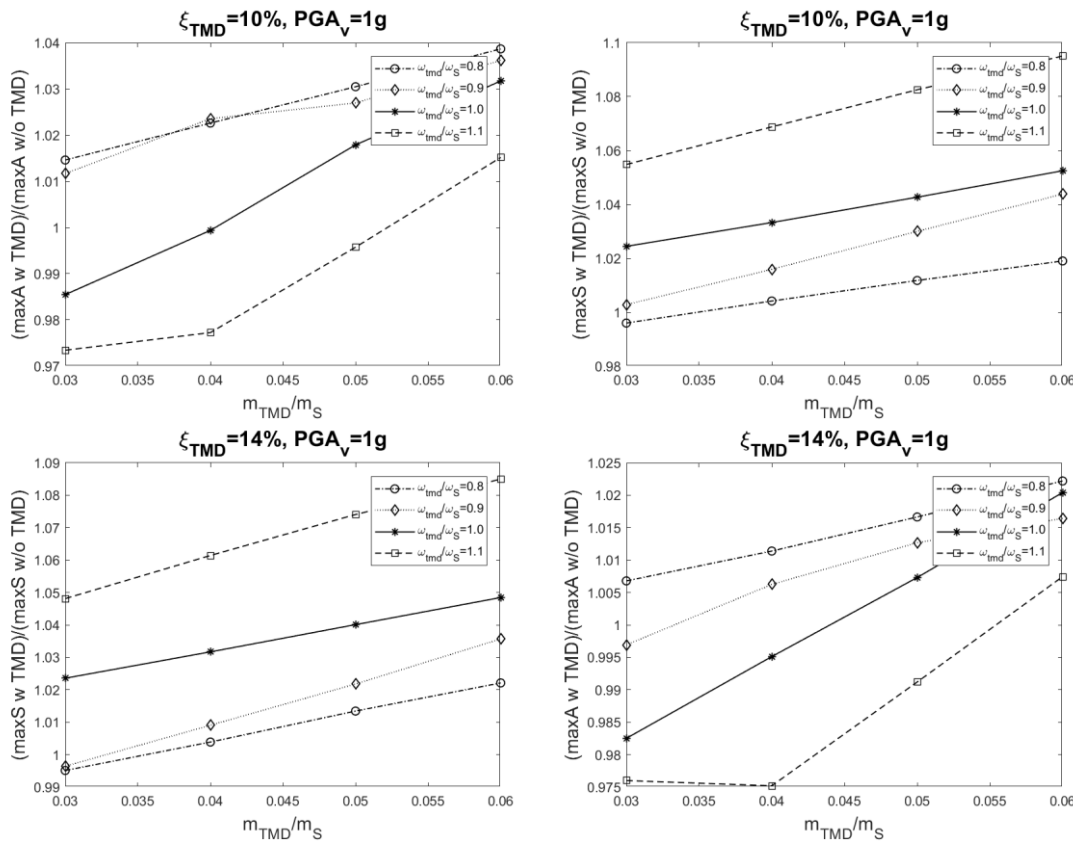

Figure 2: NPP with HDRBs (parameters from [2]): parametric study following the Den Hartog [22] tuning equations for different levels of TMD damping (ξ). Horizontal axis: TMD mass over the system mass; vertical axis: ratio between the system response with and w/o TMD; legend: ratio between the system and the TMD circular frequency.

Figure 2 reports the results of a parametric study in terms of the ratio of the response parameter of interest for the building with and without the control of vertical motion exerted by the TMD. The study follows the Den Hartog [22] tuning equations and spans different levels of TMD design parameters. The selected response parameters are the extreme value of the absolute vertical acceleration (*A*) of the superstructure, and the extreme value of its vertical relative displacement (*S*). As it can be appreciated from Figure 2, due to the already sufficiently large amount of damping provided by the HDRB devices [2], the introduction of a TMD resulted in a deterioration of the response both in terms of acceleration and displacements. However, the extensive use of low damping rubber bearings in existing structures suggests to consider the TMDs in association to natural rubber bearings [23, 24].

Figure 3 reports the results for a damping of the isolators that is 1/10th of that of Figure 2 Figure 3 depicts the outcome in terms of the same response parameters of Figure 2 obtained with a reduced intrinsic

7

damping of the rubber brearings (about 1%), highlighting the benefits that can be provided by the implementation of a TMD system.
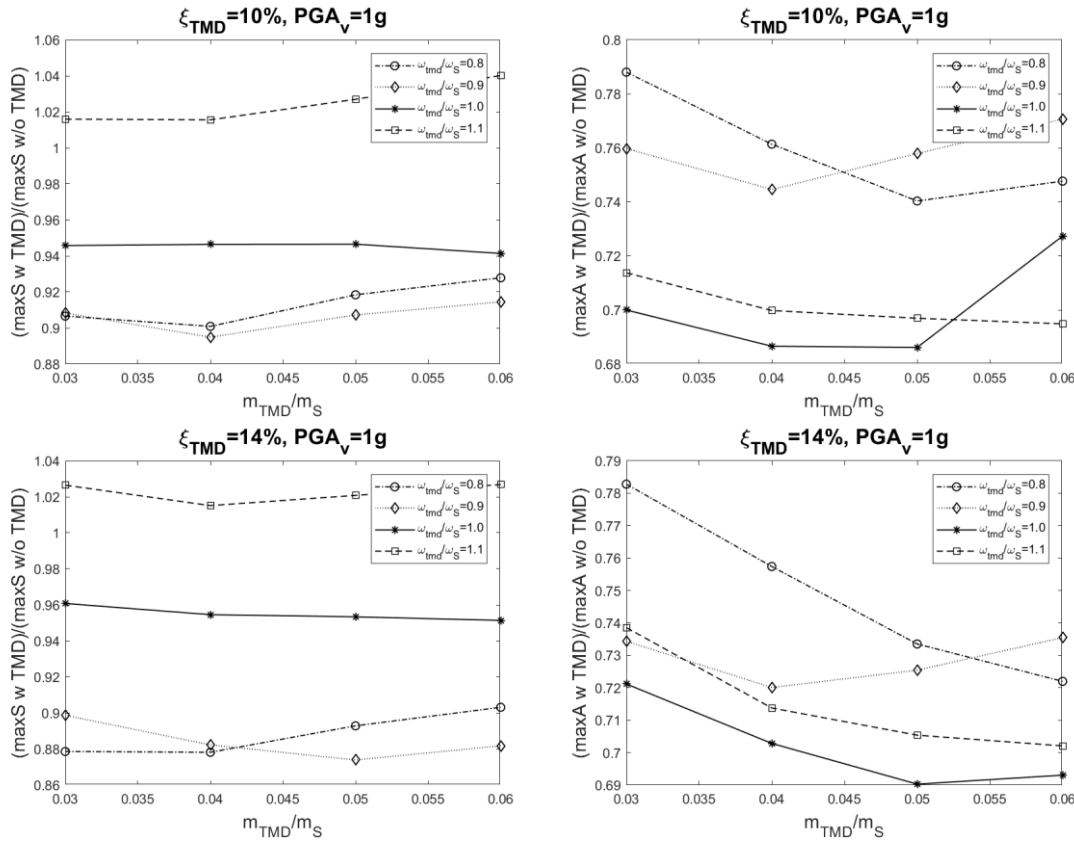

Figure 3: NPP modelled as in Figure 1 with data from [2] with reduced damping in the rubber bearings (LDRB): parametric study following the Den Hartog [22] tuning equations for different levels of TMD damping (ξ). Horizontal axis: TMD mass over the system mass; vertical axis: ratio between the system response with and w/o TMD; legend: ratio between the system and the TMD circular frequency.

5. Preliminary 3D analysis of the IRIS-NPP base isolated building with TMDs

An issue that arose in the past studies about IRIS nuclear building with base isolation [2, 17] is related to the large variation in axial forces in the same due to rocking motion sustained by the horizontal motion and the vertical distance between the NPP center of gravity and the isolation plane. In this work a preliminary 3D model (see Figure 4) of the NPP building has been developed inside the SAP2000 finite element code to address this issue. It has been studied if multiple TMDs, active exclusively in the vertical direction, are able to mitigate the rocking motion, and consequently to reduce the axial tensile force in the bearings because of the relative vertical displacement between the bearings' connection points.

Due to inherent modelling limitations, the bearings are represented though elastic-plastic spring elements (for the horizontal response) and as linear springs and dashpots (in the vertical direction). The parameters of the elastic-plastic springs have been identified on the base of the experimental outcomes in [2]. They are: elastic stiffness K_e = 20000 kN/m, yielding strength f_y = 187 kN, ratio r of post-elastic stiffness to elastic stiffness, r = 0.43. The choice of an elastic-plastic model leads to a lower energy dissipation with respect to the prototype in [2], and, as a consequence, the actual horizontal displacements are expected to be of lower value than the ones predicted by the SAP2000 numerical model (Figure 5).

8

In the vertical direction the devices are modelled with elastic springs in parallel to viscous dampers. The stiffness of the vertical spring, representing the vertical stiffness of the isolators, has been selected to match the experimental response of the tested specimen [2] ($K_v = 7884615$ kN/m). The damping constant of the viscous damper was selected to reach the nominal damping of 10% ($C_v = 14596$ kNs/m). The mass of the NPP is 81060 kNs^2/m, while the centroid inertial moments are 22039000 kNs^{2}m, 22039000 kNs^{2}m, 25331250 kNs^{2}m, respectively for I_1, I_2, I_3 (Figure 1).
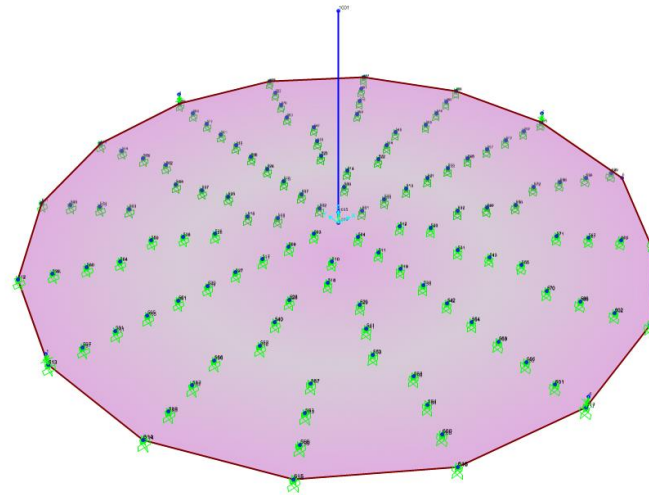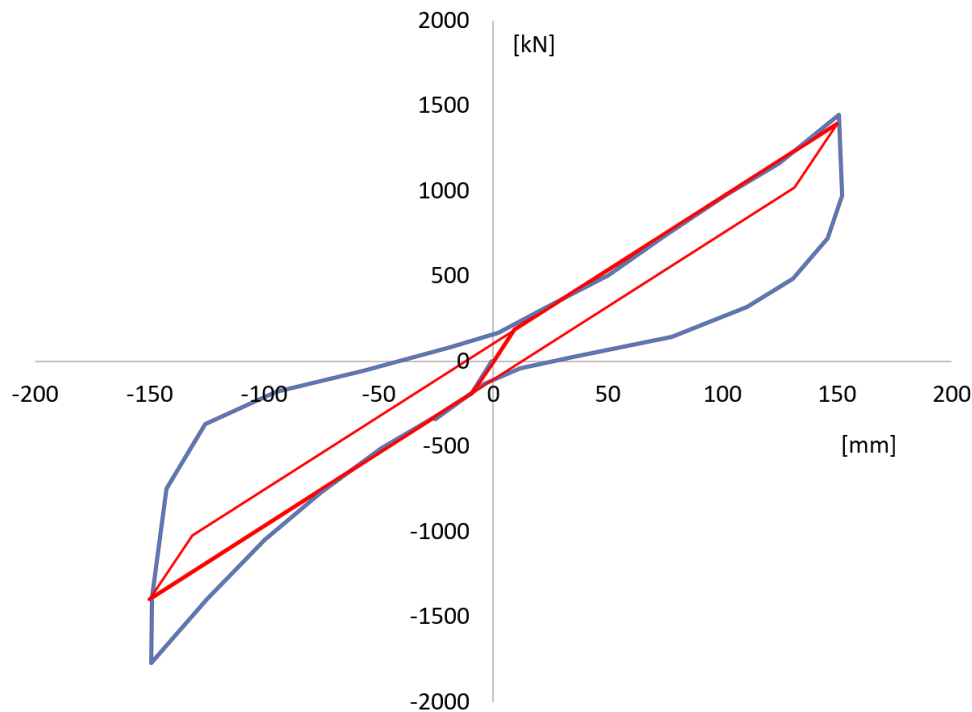

Figure 4: Preliminary SAP model

Figure 5: Hysteretic signature in SAP and comparison with the original implementation in [2]

9

The NPP building described in [2], with base isolation modelled as previously reported, has then been equipped with 5 TMD as indicated in Section 3. Each couple of TMDs at the extremities of the *x* (or *y*) axis provide 20% of the inertia moment of the whole NPP building about the other centroidal horizontal axis. The mass of each TMD results to be about 4% of the total NPP mass, while is providing 10% of the NPP inertia moment. The TMD stiffness is computed to achieve a frequency ratio of 0.97 (with respect to the horizontal isolation frequency, which is about 1.63Hz), while the damping coefficient is equal to 9105 kNs/m in order to have a damping relative to the critical of 13%. The central TMD has been designed to control the vertical motion of the NPP. It has a mass equal to 10% of the total NPP mass, a stiffness that has been selected to have a frequency ratio of 0.97 with respect to the modal frequency (about 17.1 Hz) related to the vertical oscillation of the NPP, a damping that has been set to 13% relative to the critical.

Figure 6 reports the comparison between the original isolation arrangement with HDRBs of the IRIS reactor, modelled in SAP2000, and the solution that implements the 5 TMDs in parallel. The comparison is in terms of vertical relative displacements accross the isolators at the extremities of the *x* and *y* axis. It can be noted the contribution of the TMDs in mitigating the rocking motion.

In light of the lack of consensus on the value of the damping in the axial (vertical) direction in HDRB, a new analysis has been then performed assuming a damping, relative to the critical, of 3% in the vertical direction. Figure 7 reports the comparison between the original base isolation solution for the IRIS NPP (now with 3% damping in vertical direction) and the one supplemented with 5 parallel TMDs. No reasonable difference can be noted, since the vertical motion is mainly driven by the horizontal one, and this results unchanged since only the vertical characteristic of the devices was modified.
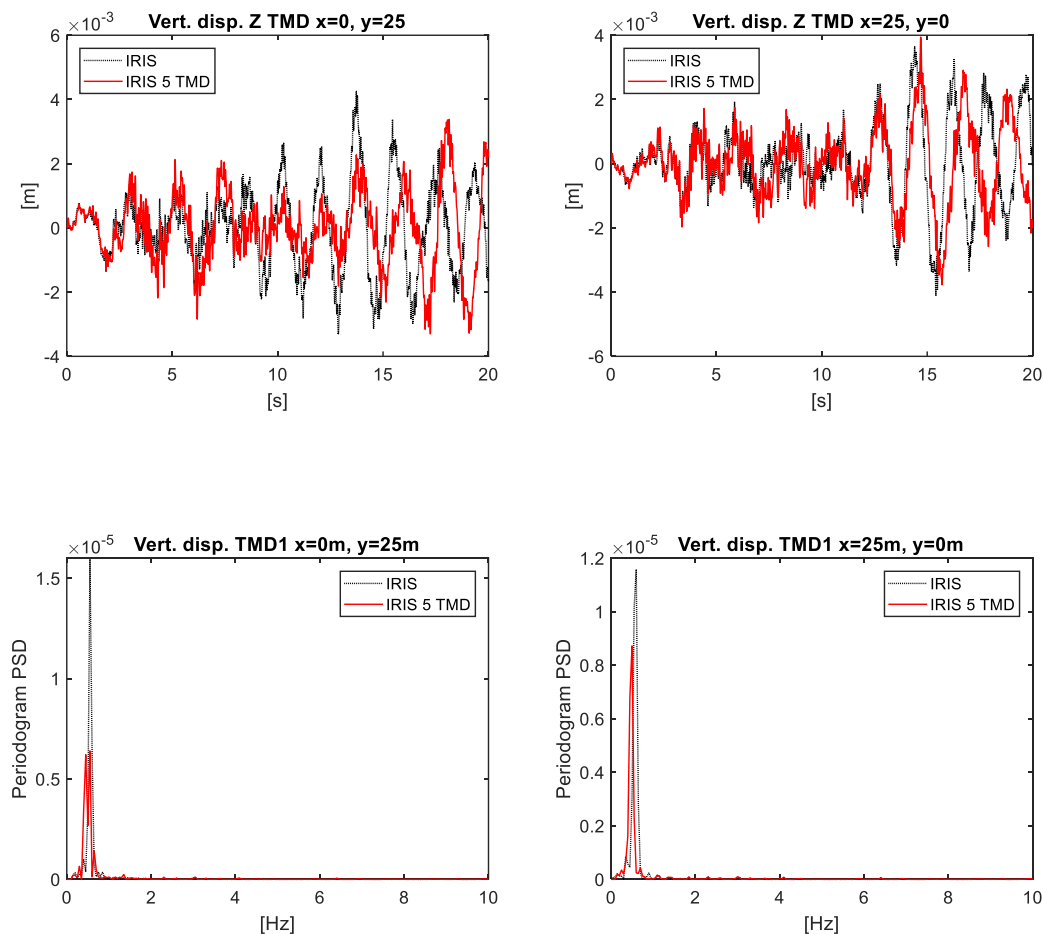

10

Figure 6 – Vertical relative displacements at the extremities of the x and y axis. Comparison between standard base isolation and 3D base isolation (5 TMDs) in SAP2000. Isolation system design as in [2]
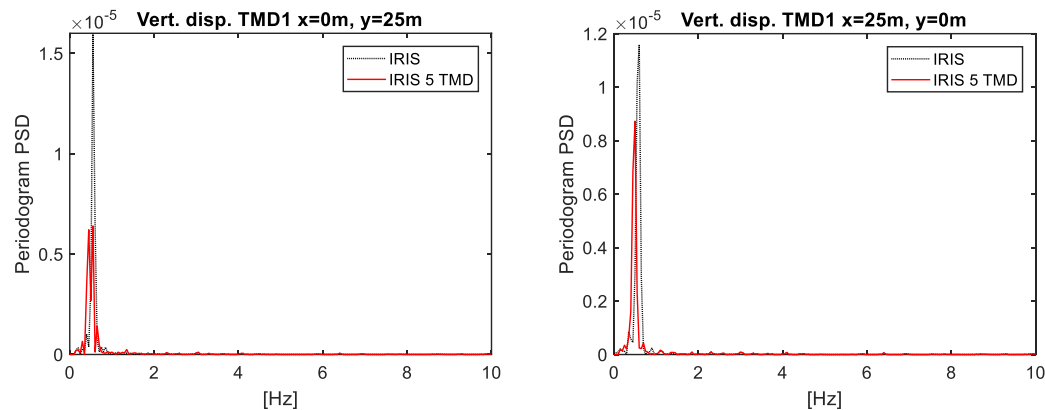

Figure 7 – Vertical relative displacements at the extremities of the x and y axis. Comparison between standard base isolation (3% damping in vertical direction) and 3D base isolation (5 TMDs) in SAP2000.

6. Conclusions

This paper deals with a preliminary study indagating the possibility to control rocking and vertical motion of base isolated NPPs which adopt rubber bearings. An innovative solution that consists in the implementation of a TMD in the vertical direction, in parallel to traditional base isolated systems, is used to mitigate the vertical response. This leads to a 3-D base isolation with uncoupled reaction components.

The results show that the implementation of TMDs can be somewhat beneficial to reduce the relative displacement across the isolation bearings and vertical absolute accelerations. However, the level of the inherent damping in the base isolation bearings drive the effectiveness of the proposed solution. Besides, when the rocking motion becomes critical, the horizontal isolation stiffness mainly affects the response.

7. Acknowledgements

8. References

[1] Domaneschi M, Martinelli L, Cattivelli C (2018): Phenomenological Model of Seismic Isolation Rubber Bearings with Variable Axial Loading. *Frontiers in Built Environment – Earthquake Engineering*, **4**, Article 49.

[2] Perotti F, Domaneschi M, De Grandis S (2013): The numerical computation of seismic fragility of base-isolated Nuclear Power Plant buildings. *Nuclear Engineering and Design*, **262**:189–200.

[3] Basu B, Bursi O, Casciati F, Casciati S, Del Grosso A, Domaneschi M, Faravelli L, Holnicki J, Irschik H, Krommer M, Lepidi M, Martelli A, Oztork B, Pozo F, Pujol G, Rakicevic Z, Rodellar J (2014). An EACS joint perspective. Recent studies in civil structural control across Europe. *Structural Control & Health Monitoring*, **21**(12): 1414–1436.

[4] Eurocode 8 EC8 (1998). UNI ENV 1998, Design of Structures for Earthquake Resistance.

[5] Tanaka et al. (1989). Development of earthquake and microtremor isolation floor system utilizing air springs and laminated rubber bearings. *IHI Engineering Review (English Edition)*, **22**(2): 47-52.

[6] Cimellaro GP, Domaneschi M, Warn G (2018). Three-Dimensional base isolation using vertical negative stiffness devices. *Journal of Earthquake Engineering*. DOI 10.1080/13632469.2018.1493004.

[7] Domaneschi M, Martinelli L, Po E (2015). Control of Wind Buffeting Vibrations in a Suspension Bridge by TMD: hybridization and robustness issues. *Computers and Structures*, 155:3-17.

[8] Den Hartog JP (1985). Mechanical Vibrations, Civil, Mechanical and Other Engineering Series, Dover Civil and Mechanical Engineering, Dover books on engineering, Courier Corporation, 1985, ISBN 0486647854, 9780486647852.

[9] Warburton GB (1982). Optimum Absorber Parameters for Various Combinations of Response and Excitation Parameters. *Earthquake Engineering & Structural Dynamics*, **10**(3):381-401.

[10] Ioi T, Ikeda K (1978). On the Dynamic Vibration Damped Absorber of the Vibration System. *Bulletin of the Japanese Society of Mechanical Engineering*, **21**(151):64-71.

[11] Asami T, Nishihara O, Baz AM (2002). Analytical Solutions to H∞ and H2 Optimization of Dynamic Vibration Absorbers Attached to Damped Linear Systems. *Transactions of the ASME*. 124:284-294.

[12] Hoang N, Fujino Y, Warnitchai P (2008). Optimal tuned mass damper for seismic applications and practical design formulas. *Engineering Structures*, **30**:707–715.

[13] Kanai K. (1975). Semi-empirical formula for the seismic characteristics of the ground. *Bulletin of the Earthquake Research Institute, The University of Tokyo*, **35**:309–25.

[14] Tajimi H (1960). A statistical method of determining the maximum response of a building structure during an earthquake. In *Proc. 2nd world conf. on earthquake engineering*, **II**:781–98.

[15] Martinelli L, Barbella G, Feriani A (2010). Modeling of Qiandao Lake submerged floating tunnel subject to multi-support seismic input. *Procedia Engineering*, **4**:311-318.

[16] Martinelli L, Barbella G, Feriani A (2011). A numerical procedure for simulating the multi-support seismic response of submerged floating tunnels anchored by cables. *Engineering Structures*, **33**:2850-2860.

[17] Tomasin M, Domaneschi M, Guerini C, Martinelli L, Perotti F (2018). A comprehensive approach to small and large-scale effects of earthquake motion variability. *Computers and Structures*, **207**:155-170.